Universal quantum criticality at finite temperature for two-dimensional disordered and clean dimerized spin-$\frac{1}{2}$ antiferromagnets

D.-R. Tan and F.-J. Jiang*

Department of Physics, National Taiwan Normal University, 88, Sec.4, Ting-Chou Rd., Taipei 116, Taiwan

(Received 11 September 2018; revised manuscript received 5 November 2018; published 10 December 2018)

The quantum critical regimes (QCR) of both a two-dimensional (2D) disordered spin-$\frac{1}{2}$ antiferromagnet and a 2D clean dimerized quantum Heisenberg model are studied using the first-principles nonperturbative quantum Monte Carlo simulations. In particular, the three well-known universal coefficients associated with QCR are investigated in detail. While in our investigation we find the obtained results are consistent with the related analytic predictions, non-negligible finite-temperature (T) effects are observed. Moreover, a striking finding in our study is that the numerical value for one of the universal coefficients we determine is likely to be different significantly from the corresponding (theoretical) result(s) established in the literature. To better understand the sources for the discrepancy observed here, apart from carrying out the associated analytic calculations not considered previously, it will be desirable as well to conduct a comprehensive examination of the exotic features of QCR for other disordered and clean spin systems than those investigated in this study.

DOI: 10.1103/PhysRevB.98.245111

I. INTRODUCTION

The two-dimensional (2D) quantum antiferromagnets, both with and without charge carriers, are among the most important systems in condensed matter physics. From the experimental perspective, these materials are related to the high-temperature (high-T_c) cuprate superconductors. As a result, numerous associated experiments were conducted and the obtained data have triggered many theoretical studies of these systems, including accurate determination of their low-temperature properties such as the staggered magnetization density and the spin stiffness [1–11].

Theoretically, at zero temperature and in the ordered phase, the 2D spin-$\frac{1}{2}$ Heisenberg antiferromagnet can be mapped to a classical system with the effects of quantum fluctuations being transformed into the renormalization of couplings [1,3]. This region is known as the renormalized classical regime in the literature. When the long-range order of the system is destroyed by the quantum fluctuations, a completely different portrait of its ground states called the quantum disordered regime appears. Moreover, in both regimes, as the temperature T rises, there will be crossovers such that the system enters yet another unique phase called the quantum critical regime (QCR). In particular, due to the interplay between the thermal and the quantum fluctuations, some exotic characteristics will emerge in QCR. These special features of QCR are signaled out by the presence of several universal behaviors among some physical quantities of the underlying 2D spin system [12–15].

Based on the analytic calculations using the method of large-N expansion for the effective nonlinear sigma model of the 2D Heisenberg antiferromagnet, three universal relations are established (assuming the dynamic exponent z is 1): $\chi_u = \frac{\Omega}{c^2}T$, $S(\pi,\pi)/\chi_s = \Xi T$, and $c/\xi = XT$. Here, χ_u, c, $S(\pi,\pi)$, χ_s, and ξ are the uniform susceptibility, the spin wave velocity, the staggered structure factor, the staggered susceptibility, and the correlation length, respectively. Moreover, the coefficients Ω, Ξ, and X are universal, namely, their numerical values are independent of any microscopic details. For 2D dimerized Heisenberg models with spatial anisotropy, QCR as well as the related universal coefficients should be detectable at any values of the corresponding tuning parameter. It is probable as well that systems with (certain kinds of) quenched disorder may exhibit features of QCR.

Interestingly, while universal behavior characterizing QCR is indeed observed for several numerical studies of 2D dimerized spin models, crystal clear evidence is only found at the finite-temperature regions above the related quantum critical points (QCPs). In other words, when the associated calculations are conducted away from QCPs, the emergence of the exotic QCR scaling has not been established rigorously and numerically yet [16–21]. For example, as introduced in the previous paragraph regarding QCR, a plateau is supported to appear in a certain region of the inverse temperature β when $S(\pi,\pi)/(\chi_s T)$ is treated as a function of β. However, such a scenario does not occur in the relevant studies when the used data were determined away from the corresponding QCPs.

At the moment, numerical studies related to QCR have been focusing on clean dimerized spin systems. The exploration of whether features of QCR, in particular the three universal quantities mentioned previously, exist for models with quenched disorder have been examined only implicitly, not systematically. Motivated by this, here we simulate a 2D spin-$\frac{1}{2}$ Heisenberg model on the square lattice with a kind of (quenched) disorder using the quantum Monte Carlo (QMC) calculations. The employed disorder distribution is based on the so-called configurational disorder introduced in Ref. [22]. Apart from this, the 2D clean dimerized plaquette

*fjjiang@ntnu.edu.tw

quantum spin system is investigated as well for comparison and clarification.

Remarkably, for both the considered disordered and clean models, features of QCR do emerge at their corresponding QCPs. Furthermore, non-negligible T dependence for the universal quantities of QCR, which was overlooked before, is found in our investigation. The most striking result obtained here is that the numerical values of the universal coefficient Ω determined in our study for both the considered models are likely to deviate significantly from those calculated previously in Refs. [15,18,19,21]. The evidence provided here for the described variation regarding the numerical value of Ω is convincing. This finding of ours is consistent with that obtained in Ref. [23]. Specifically, in Ref. [23] the Ω calculated through a detailed study of a 2D clean bilayer quantum spin system differs considerably from the known numerical results in the literature. To better understand the sources of the discrepancy found here, apart from carrying out the analytic calculations associated with corrections not taken into account previously, a more thorough exploration of other disordered and clean spin models than those studied here is desirable.

The rest of the paper is organized as follows. After the Introduction, the considered models as well as the required physical quantities for investigating the features of QCR are described. A detailed analysis, focusing on the three well-known universal coefficients of QCR, is presented then. In particular, the numerical evidence for the discrepancy mentioned above is given. Finally, a section is devoted to conclude our study shown here.

II. MICROSCOPIC MODEL AND OBSERVABLES

The 2D spin-$\frac{1}{2}$ system with a quenched disorder and the 2D clean quantum dimerized plaquette Heisenberg model studied here are given by the same form of Hamilton operator

$$H = \sum_{\langle ij \rangle} J_{ij}\, \vec{S}_i \cdot \vec{S}_j + \sum_{\langle i'j' \rangle} J'_{i'j'}\, \vec{S}_i \cdot \vec{S}_j, \tag{1}$$

where J_{ij} and $J'_{i'j'}$ are the antiferromagnetic couplings (bonds) connecting nearest-neighbor spins $\langle ij \rangle$ and $\langle i'j' \rangle$, respectively, and $\vec{S}_i$ is the spin-$\frac{1}{2}$ operator at site i. The quenched disorder considered in this investigation is based on the idea of configurational disorder [22]. Specifically, in our simulations for the disordered model, the probabilities of putting a pair of J' bonds vertically and horizontally in a plaquette consisting of two by two spins are both 0.5. (We will still use the term configurational disorder for this employed disorder distribution in the rest of the paper.) Figure 1 demonstrates the studied disordered and clean models. Here, we use the convention that the couplings J' and J satisfy $J' > J$. As a result, each of the considered system will undergo a quantum phase transition once the ratio J'/J exceeds a particular value called the critical point. These special points in the associated parameter spaces are commonly denoted by $(J'/J)_c$ in the literature.

To examine the well-known universal relations of QCR, particularly to understand whether these relations appear for the considered disordered system, the staggered structure factor $S(\pi, \pi, L)$, the uniform and staggered susceptibilities (χ_u and χ_s), the spin wave velocity c, as well as the correlation length ξ are measured. The staggered structure factor $S(\pi, \pi, L)$ on a finite lattice with a linear box size L is defined by

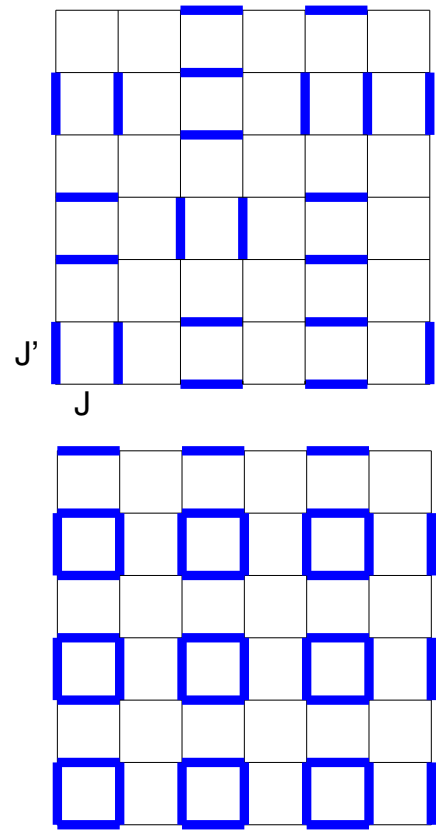

FIG. 1. The model with configurational disorder (top panel) and the clean dimerized plaquette model (bottom panel) considered in this study.

$$S(\pi, \pi, L) = 3L^2 \left\langle \left(m_s^z\right)^2 \right\rangle, \tag{2}$$

where $m_s^z = \frac{1}{L^2} \sum_i (-1)^{i_1+i_2} S_i^z$ and the summation is over all sites. The uniform susceptibility χ_u and staggered susceptibility χ_s take the forms

$$\chi_u = \frac{\beta}{L^2} \left\langle \left(\sum_i S_i \right)^2 \right\rangle \tag{3}$$

and

$$\chi_s = 3L^2 \int_0^\beta \left\langle m_s^z(\tau) m_s^z(0) \right\rangle d\tau, \tag{4}$$

respectively. The quantity β appearing above is the inverse temperature. In addition, the correlation length ξ is expressed as

$$\xi = \frac{L_1}{4\pi} \sqrt{\frac{S(\pi,\pi)}{S(\pi + 2\pi/L_1, \pi)} - 1} + \frac{L_2}{4\pi} \sqrt{\frac{S(\pi,\pi)}{S(\pi, \pi + 2\pi/L_2)} - 1}, \tag{5}$$

where the quantities $S(\pi + 2\pi/L_1, \pi)$ and $S(\pi, \pi + 2\pi/L_2)$ are the Fourier modes with the second largest magnitude.

Finally, the spin wave velocities c for both the investigated models are calculated through the temporal and spatial winding numbers squared ($\langle W_t^2\rangle$ and $\langle W_i^2\rangle$ with $i \in \{1, 2\}$).

We would also like to point out that while the same notations are used here for both the observables of the two studied spin systems, whenever a physical quantity associated with the disordered model is presented, it is obtained by averaging over the generated configurations of randomness.

III. NUMERICAL RESULTS

To study the features of QCR associated with the considered disordered and clean models, we have performed large-scale QMC simulations using the stochastic series expansion (SSE) algorithm with very efficient operator-loop update [24]. For the disordered quantum spin system, while most of the corresponding results presented here are obtained by averaging over several hundred realizations of randomness, the outcomes related to the spin wave velocity are calculated using (a) few thousand disorder configurations.

For a given J'/J and for the corresponding results of finite T, a generated configuration of randomness is employed for the calculations associated with several sequential values of β. Furthermore, for (almost) every considered temperature at least 5000 Monte Carlo (MC) sweeps as well as the step of adjusting cutoff in the SSE algorithm are carried out for both the processes of thermalization and measurement. Therefore, the correlations among the obtained data are anticipated to be mild. In particular, the first few data in a Monte Carlo simulation are disregarded for the disorder average. As a result, the potential issue of thermalization in studies of disordered systems is under control. Indeed, the outcomes resulting from several additional calculations using 2500 MC sweeps for the thermalization agree remarkably well with those explicitly shown here.

We would also like to emphasize the fact that the uncertainties of the calculated observables should be dominated by the number of configurations used for the disorder average. This is because for each considered set of parameter, the number of MC sweeps employed for the related simulations is much larger than that of the associated configurations generated. Still, the errors for the obtained quantities are estimated with conservation so that the statistical uncertainties resulting from the MC simulations are not overlooked. In addition, most (a few) of the results presented here are obtained on $L = 256$ ($L > 256$) lattices. For comparison, some outcomes determined with smaller box sizes are shown as well. Finally, it should be pointed out that in this study, whenever a presented numerical result is obtained by fitting the associated data, the quoted number is based on the fits that satisfy $\chi^2/\mathrm{DOF} < 2$.

To carry out a comprehensive (and detailed as well) study of QCR for the investigated models, ideally the calculations should be conducted at the associated QCPs. In theory, close to a second-order quantum phase transition and for various L and (J'/J), if one treats the results of data collapse of $Q_2/(1 + aL^{-\omega})$ as functions of $[(j - j_c)/j_c]L^{1/\nu}$, then a universal smooth curve should emerge. Here, $j = J'/J$, $j_c = (J'/J)_c$, ν and ω are the correlation length and the confluent critical exponents, respectively, and a is some constant. Moreover, Q_2 is the second Binder ratio which is defined by $Q_2 = \frac{\langle (m_s^z)^4\rangle}{\langle (m_s^z)^2\rangle^2}$. Interestingly, the zero-temperature data we calculate with the β-doubling scheme [25] are fully consistent with the outcomes reached in Ref. [22]. Indeed, using $a = -0.5$, $\omega = 1.0$, $j_c = 1.990$ (these three results are taken directly from Ref. [22]), $\nu = 0.7115$ (the established value for this exponent), as well as the data obtained here, we have reproduced the associated universal curve of Q_2 just like the one shown in Ref. [22] (see Fig. 2). With a fixed $\nu = 0.7115$, we additionally fit the observables Q_2 and $\rho_s L$ [26] to their expected scaling formulas near QCP. The $(J'/J)_c$ determined from these fits associated with Q_2 and $\rho_s L$ are both given by $(J'/J)_c = 1.990(1)$. This strongly suggests that taking 1.990(1) as the QCP for the investigated disordered model should be beyond any doubt.

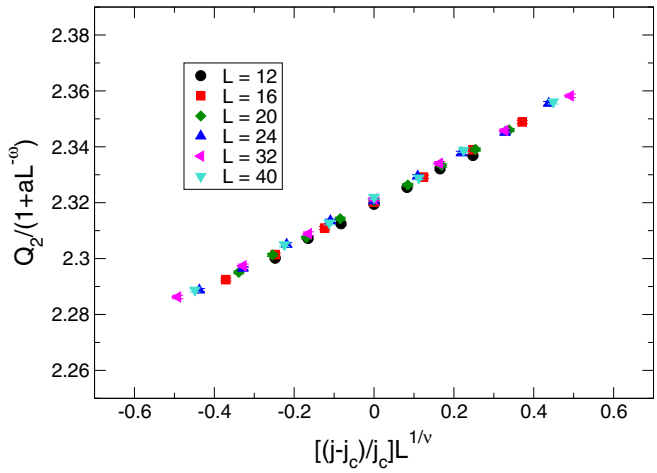

FIG. 2. $Q_2/(1 + aL^{-\omega})$ (of the studied disordered model) as functions of $[(j - j_c)/j_c]L^{1/\nu}$ for various L and J'/J. Here, j and j_c are defined as $j = J'/J$ and $j_c = (J'/J)_c$, respectively. While the numerical values of the coefficients $a = -0.5$, $\omega = 1.0$, and $j_c = 1.990$ are taken directly from the outcomes determined in Ref. [22], the ν used in producing the universal curve is its theoretical prediction $\nu = 0.7115$.

While it is desirable to simulate larger lattices (and obtain more data points) in order to have a better estimation of $(J'/J)_c$, as we will demonstrate later, with the accuracy of the $(J'/J)_c$ employed here, namely $(J'/J)_c = 1.990(1)$, we are able to obtain unambiguous conclusions and results regarding the considered universal coefficients. Apart from this, as will be shown as well in the relevant section, the numerical value of Ω estimated from the studied clean plaquette model, which has a precisely determined critical point $(J'/J)_c = 1.8230(2)$, is in nice agreement with that of the investigated disordered system (see Figs. 8 and 11). This suggests that the critical point $(J'/J)_c = 1.990(1)$ used here for the disordered model is accurate.

The fact that the $(J'/J)_c$ resulting from Q_2 and $\rho_s L$ agree quantitatively with each other indicates that the dynamic exponent z related to the considered disordered system is 1. We will demonstrate shortly that this is truly the case. Finally, the QCP of the clean plaquette model has been calculated in Ref. [27] and is given by $(J'/J)_c = 1.8230(2)$.

A. Determination of spin wave velocity c

The spin wave velocities c at the critical points for the studied models are calculated using the method of winding numbers squared proposed in Refs. [23,28]. Specifically, for a fixed box size L (and a fixed J'/J), the value of β is adjusted in the calculations so that the temporal winding number squared $\langle W_t^2\rangle$ agrees quantitatively with that of the averaged spatial winding numbers squared $\langle W^2\rangle = \frac{1}{2}\sum_{i=1,2}\langle W_i^2\rangle$. Under such a condition, the corresponding spin wave velocity $c(L, J'/J)$ is determined by the equation $c(L, J'/J) = L/\beta^\star$, where $\beta^\star$ is the inverse temperature for which the condition described above regarding the winding numbers squared is fulfilled. Since this method is valid only when the long-range antiferromagnetic order is present in the system, the relevant simulations are done at $J'/J = 1.988$ for the disordered system [which has $(J'/J)_c = 1.990(1)$ [22]]. For the clean plaquette model, calculations at several selected $J'/J < (J'/J)_c = 1.8230(2)$, as well as fits and interpolations, are conducted in order to obtained the bulk c at the associated critical point.

1. Spin wave velocity of the disordered system

The $\langle W_t^2\rangle$ and $\langle W^2\rangle$ as functions of β for the studied disordered system are shown in Fig. 3. The calculations are done at $J'/J = 1.988$ and the outcomes presented in the top and bottom panels of the figure are obtained with $L = 24$ and 48, respectively. The corresponding values of c estimated conservatively from these two simulated results match each other nicely. Indeed, while the calculated result of c for $L = 24$ is given by $c = 1.934(5)J$, the c determined from the data of $L = 48$ is found to be $c = 1.931(9)J$. We have additionally performed simulations at $J'/J = 1.986$ with $L = 48$. The outcome of c from the simulations associated with $J'/J = 1.986$ agrees remarkably well with that of $J'/J = 1.988$. Therefore, it should be accurate to use $c = 1.931(9)J$ as the bulk value of c right at the critical point.

2. Spin wave velocity of the clean plaquette model

To determine the bulk c at the critical point of the 2D clean plaquette model, a more thorough calculation is performed. In particular, we carry out simulations with various box sizes L at several selected $J'/J \leqslant 1.8227$ close to the critical point $(J'/J)_c = 1.8230(2)$. The obtained results are shown in Fig. 4. The bulk $c(J'/J)$ of each considered J'/J is determined by applying the following two *Ansätze*

$$a_0 + a_1/L^2, \tag{6}$$

$$b_0 + b_1/L^2 + b_2/L^3 \tag{7}$$

to fit the corresponding data. This strategy of calculating the bulk values of c is inspired by the results demonstrated in Ref. [23]. The uncertainty for the bulk c of every used J'/J is the standard deviation deriving from considering Gaussian noises in the associated weighted χ-squared fits. With the outcomes from the fits employing *Ansatz* (7), the c corresponding to $(J/'J)_c$ is estimated by interpolation based on a linear fit of the form $a(J'/J) + b$. With such a procedure, the spin wave velocity c at the critical point is found to be $c = 2.163(4)J$.

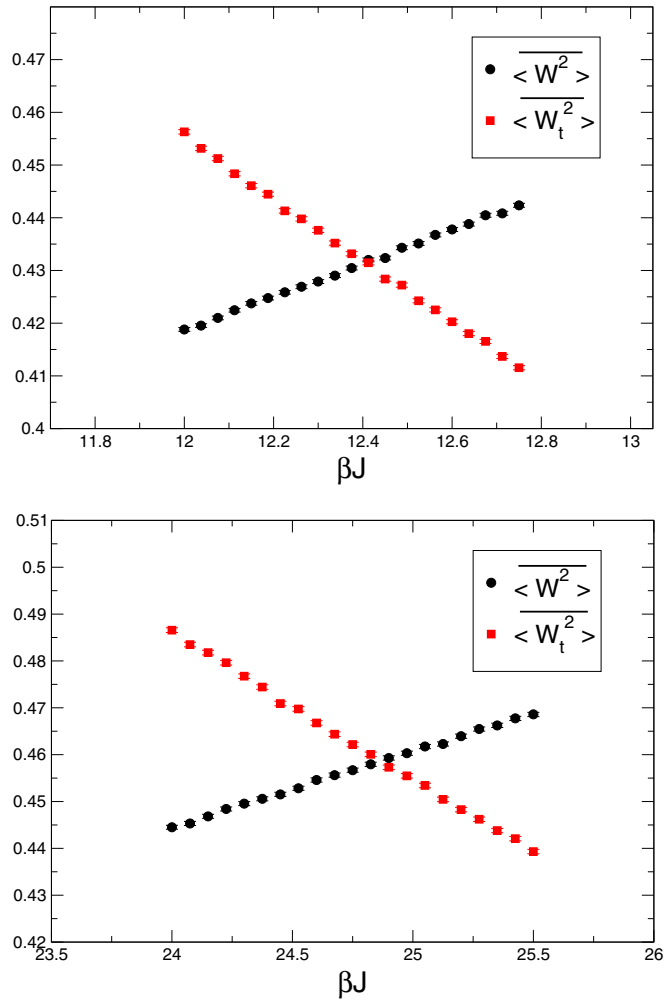

FIG. 3. The temporal and spatial winding numbers squared as functions of β for the studied disordered model. The simulations are conducted at $J'/J = 1.988$ and the results shown in the top and the bottom panels are determined with $L = 24$ and 48, respectively.

Here, the quoted uncertainty is not determined directly from the interpolation, but is calculated with conservation assuming that for $(J'/J)_c$ a similar statistic as those of the J'/J shown in Fig. 4 is reached.

B. Universal coefficient Ω

Theoretically, the universal coefficient Ω is given by $\chi_u = (\Omega/c^2)T^{d/z-1}$ at the critical point, where d is dimensionality of the system (which is 2 here) and z is the associated dynamic exponent. The z corresponding to the considered disordered model is estimated to be 1 in Ref. [22].

1. Results of disordered system

The $\chi_u c^2$ [determined at $(J'/J)_c = 1.990$ and on $L = 256$ lattices] as a function of T for the studied 2D spin-$\frac{1}{2}$ system with configurational disorder is depicted in Fig. 5. Apart from the results obtained at the critical point $(J'/J)_c$, we have additionally performed simulations at $J'/J = 1.989$ and 1.991 with $L = 256$ so that for the considered observables

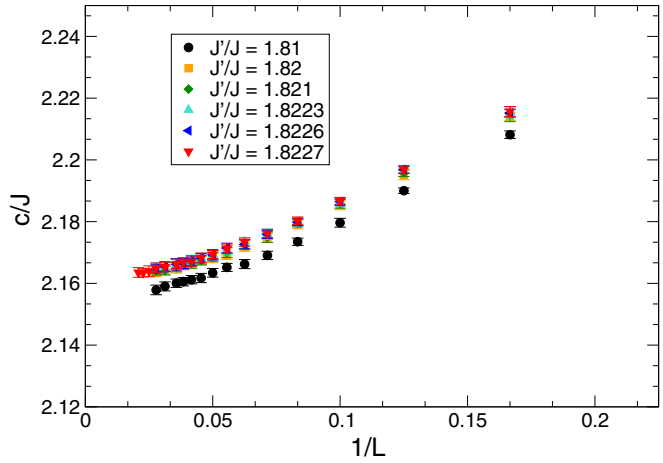

FIG. 4. The estimated c as functions of $1/L$ for several selected J'/J of the 2D plaquette model.

the corresponding systematic errors due to the uncertainty of $(J'/J)_c$ can be investigated.

The fits carried out here for the determination of Ω are done by fitting the data of $\chi_u c^2$ to both the *Ansätze*

$$a + b\,T^{2/z-1}, \tag{8}$$

$$b_1\,T^{2/z_1-1} \tag{9}$$

with a, b, b_1, z, and z_1 left as the fitting parameters. With these two formulas, the numerical values of Ω are just the parameters b and b_1 calculated from the fits. In the following, z and b, instead of z_1 and b_1, will be used whenever the results from the fits employing the second *Ansatz* are discussed, if no confusion arises.

The obtained results of z and b for all the three considered values of J'/J are demonstrated in Figs. 6 (using the first *Ansatz*) and 7 (using the second *Ansatz*). The horizontal (x) axes in these figures stand for the minimum values of β used in the fits. Interestingly, as one can see from the figures, most of the determined values of z are slightly above 1. Moreover,

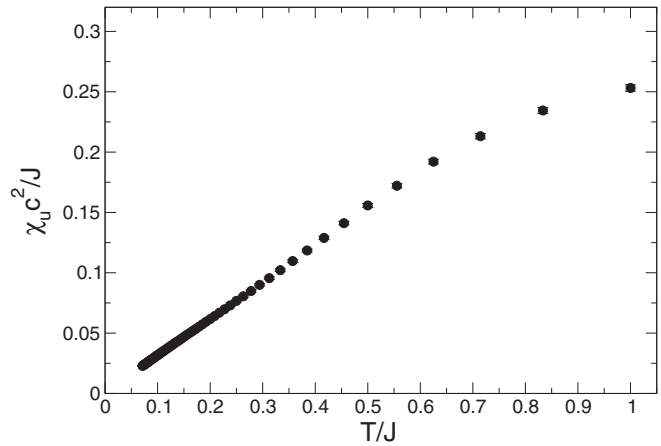

FIG. 5. $\chi_u c^2$ as a function of T for the considered disordered model. The data are obtained at the critical point $(J'/J)_c = 1.990$ with $L = 256$.

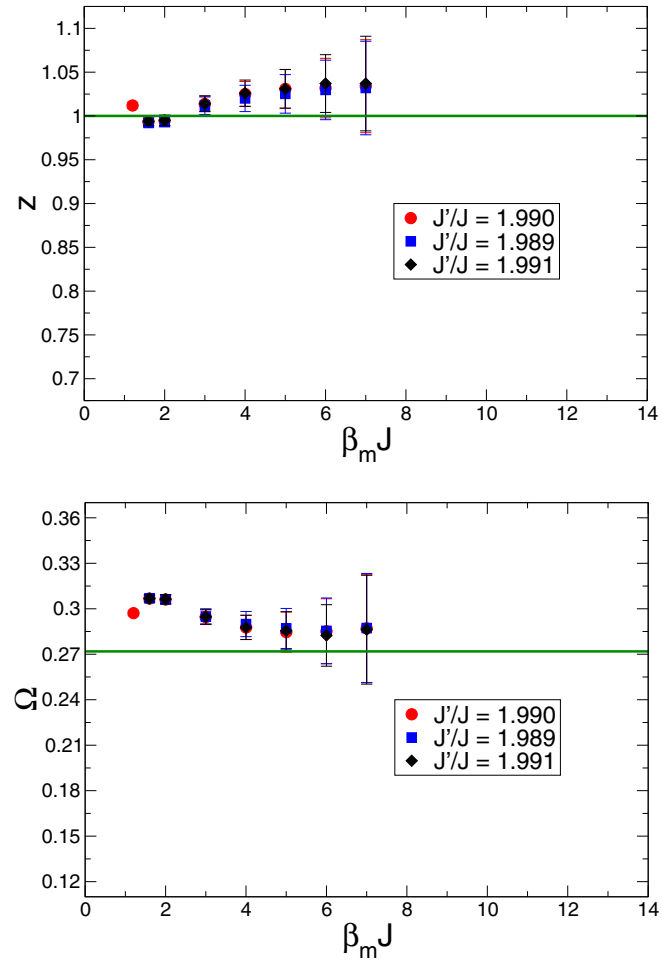

FIG. 6. The results of z (top panel) and b (Ω, bottom panel) for the considered disordered system. These outcomes are obtained from the fits using the *Ansatz* $a + b\,T^{2/z-1}$. The horizontal (x) axes stand for the minimum values of β used in the fits. The solid lines in both panels are the corresponding theoretical predictions.

the calculated b are larger than 0.271 85 (solid horizontal lines in the bottom panels of both Figs. 6 and 7). Although b is approaching 0.271 85 when more data determined at high-temperature region are excluded in the associated fits using the first *Ansatz*, the majority of the obtained results of b are well above the corresponding theoretical prediction $\Omega = 0.271\,85$. Similar to the analysis for the spin wave velocity c, here the errors shown in the figures are the standard deviations resulting from considering Gaussian noises in the related weighted χ-squared fits. While not presented here, the a determined from the fits are either with small magnitude (of the order 10^{-3}) or are statistically identical to zero.

It is intriguing to notice that when the first *Ansatz* is considered, as the magnitude of the determined z increases (this occurs when more and more data calculated at high temperatures are excluded in the fits), the value of b obtained comes toward 0.271 85. In other words, z and Ω are correlated. Since the difference between the z found here and that estimated in Ref. [22] is only at few percent level, it is unlikely that such deviations are due to the fact that the z calculated here for the studied disordered model is a new one other than

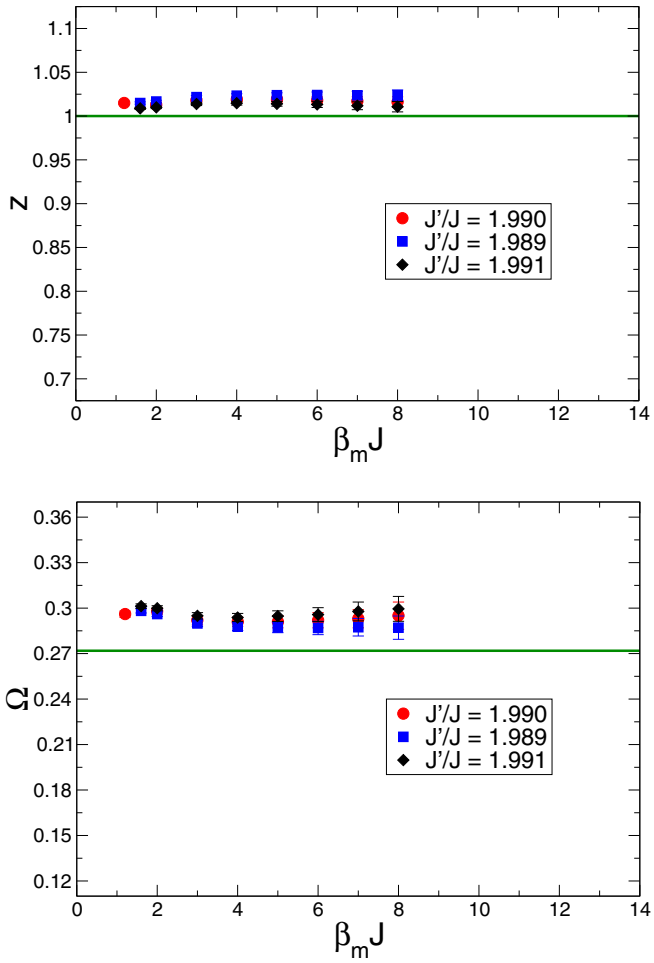

FIG. 7. The results of z (top panel) and b (Ω, bottom panel) for the considered disordered system. These outcomes are obtained from the fits using the *Ansatz* $b\,T^{2/z-1}$. The horizontal (x) axes stand for the minimum values of β used in the fits. The solid lines in both panels are the corresponding theoretical predictions.

that found in [22]. Instead, the observed discrepancy should be treated as a result of not taking some corrections into account in the analysis. Indeed, to the best of our knowledge, we are not aware of other formulas aside from those employed here for the fits. As we will demonstrate later, such a scenario for z and Ω occurs for the clean plaquette model as well.

Since $z = 1$ is beyond doubt for the considered disordered system, to accurately estimate the numerical value of Ω, particularly to understand its dependence on (finite) temperature, it is helpful to investigate the quantity $\chi_u c^2/T$ as a function of the inverse temperature β. Such a study is inspired by the fact that according to the relevant theoretical prediction, at $(J'/J)_c$ a flat plateau should appear if the data of $\chi_u c^2/T$ are plotted against β since $z = 1$. By considering the same relations, i.e.. $\chi_u c^2/T$ versus β, for other values of J'/J near $(J'/J)_c$, one can additionally estimate the associated uncertainty of Ω as well.

Remarkably, a very flat plateau indeed emerges when $\chi_u c^2/T$ is treated as a function of β (see Fig. 8). While it is

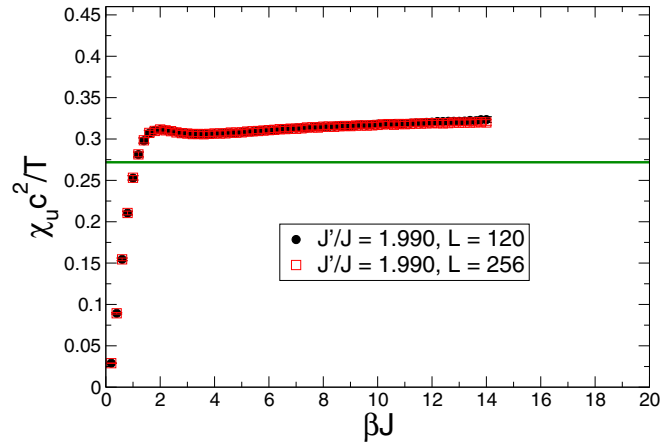

FIG. 8. $\chi_u c^2/T$ as functions of β for the studied disordered model. The data are calculated at the critical point $(J'/J)_c = 1.990$ with $L = 120$ and 256. The horizontal solid line is the theoretical prediction ~0.271 85.

clear that the quantity $\chi_u c^2/T$ receives mild corrections from terms taking some forms in T, the quality of flatness shown in Fig. 8 strongly indicates that the value of the universal coefficient Ω is larger than 0.271 85 (which is the horizontal line in Fig. 8). The $L = 120$ data of $\chi_u c^2/T$ obtained at $(J'/J)_c$ are demonstrated in Fig. 8 as well. The quantitative agreement between the $\chi_u c^2/T$ data of $L = 120$ and 256 rules out the possibility that the deviations of Ω and z from their expected values are due to finite-size effects. This strategy of confirming the obtained results are the bulk ones is as effective as other methods such as carrying out a careful finite-size analysis.

Aside from the results associated with $(J'/J)_c$, the $\chi_u c^2/T$ as functions of β for both $J'/J = 1.989$ and 1.991 are shown in Fig. 9. As can been seen from the figure, flat plateaus well above 0.271 85 show up as well. The results presented in Fig. 9 exclude the scenario that the observed discrepancy is due to the uncertainty of the critical point.

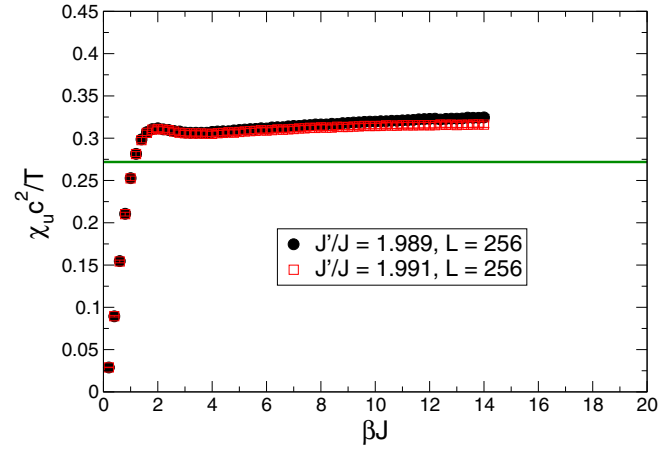

FIG. 9. $\chi_u c^2/T$ as functions of β for the studied disordered model. The data are calculated at $J'/J = 1.991$ and 1.989 with $L = 256$. The horizontal solid line is the theoretical prediction ~0.271 85.

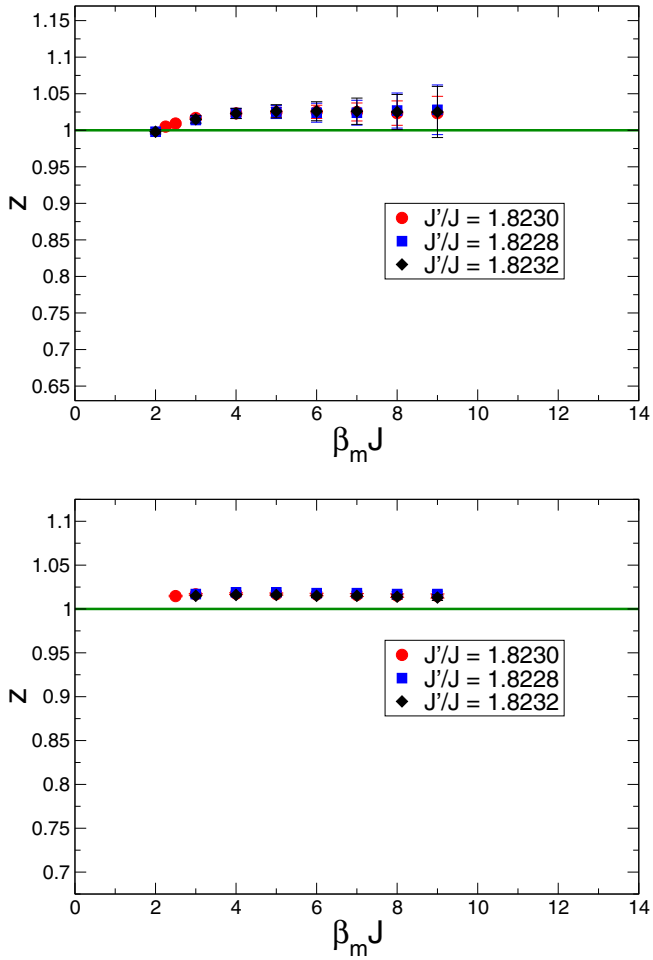

FIG. 10. The results of z for the clean plaquette model. These outcomes are obtained from the fits using the *Ansätze* $a + b\,T^{2/z-1}$ (top panel) and $b_1\,T^{2/z_1-1}$ (bottom panel). The horizontal (x) axes stand for the minimum values of β used in the fits.

2. Results of clean system

While it is well established that $z = 1$ for the considered 2D plaquette model, it will be useful to conduct a calculation like that done in the previous subsection to determine the dynamic exponent z associated with the studied clean system. Interestingly, a scenario like the one of the investigated disordered model is observed. Specifically, the values of z obtained here are slightly above the theoretical prediction $z = 1$ (see Fig. 10). Just like what has been argued previously, since the deviations found are only at few percent level, these deviations should be treated as consequences resulting from (minor) corrections not taken into account in the analysis.

Similar to the analysis done previously, we have also investigated the size-convergence quantity $\chi_u c^2/T$ as a function of β for the 2D clean dimerized plaquette model [29]. The considered data are determined at the expected critical point $(J'/J)_c = 1.8230$, as well as at $J'/J = 1.8228$, 1.8232 in order to take into account the effects from the uncertainties of $(J'/J)_c$. The resulting outcomes are depicted in Figs. 11 and 12.

Interestingly, while moderate T dependence for $\chi_u c^2/T$ definitely appears, as shown in the figures, one sees clearly

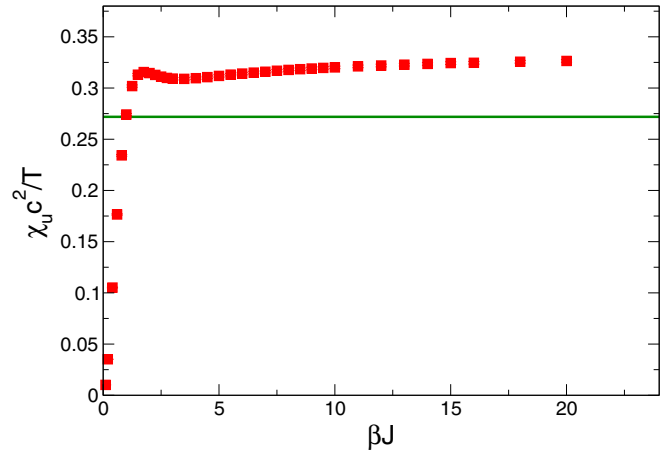

FIG. 11. Size-convergence $\chi_u c^2/T$ as a function of β for the studied 2D dimerized plaquette model. The data are calculated at the critical point $(J'/J)_c = 1.8230$ and the horizontal solid line is the theoretical prediction ∼0.271 85.

that flat plateaus emerge as well. Furthermore, by comparing the results presented in Figs. 8, 9, 11, and 12, the values of $\chi_u c/T^2$ for which all the plateaus take place match each other very well and are statistically above 0.271 85.

In summary, the outcome obtained here that Ω is quantitatively different from its theoretical prediction 0.271 85 is convincing. In particular, based on the results of fits with a fixed $z = 1$ [in the formula (8)], the numerical value of Ω we estimate conservatively is about 0.306(10). A (slightly) larger number is reached if one uses the outcomes calculated by considering only the lower-temperature data for the fits. In addition to this numerical result of Ω [$\Omega = 0.306(10)$] determined from the fits, a reasonable estimation for Ω, which is $\Omega \sim 0.32(1)$, can arise from investigating the plateau behavior of $\chi_u c^2/T$ (as functions β). Both approaches lead to values of Ω that are statistically different from 0.271 85. To arrive at a more accurate determination of Ω requires better

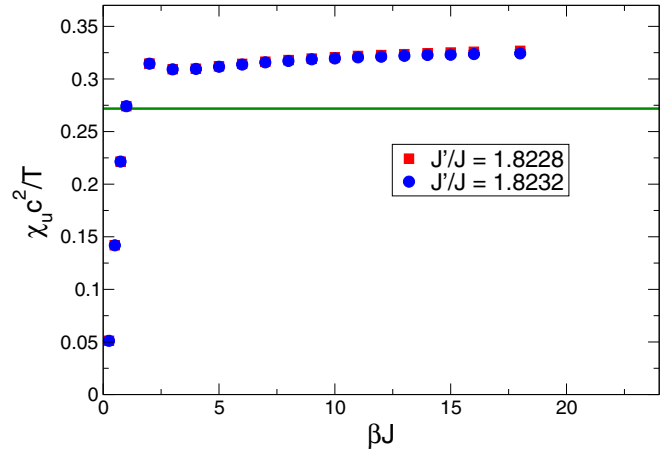

FIG. 12. Size-convergence $\chi_u c^2/T$ as functions of β for the studied 2D dimerized plaquette model. The data are calculated at $J'/J = 1.8228$ and 1.8232. The horizontal solid line is the theoretical prediction ∼0.271 85.

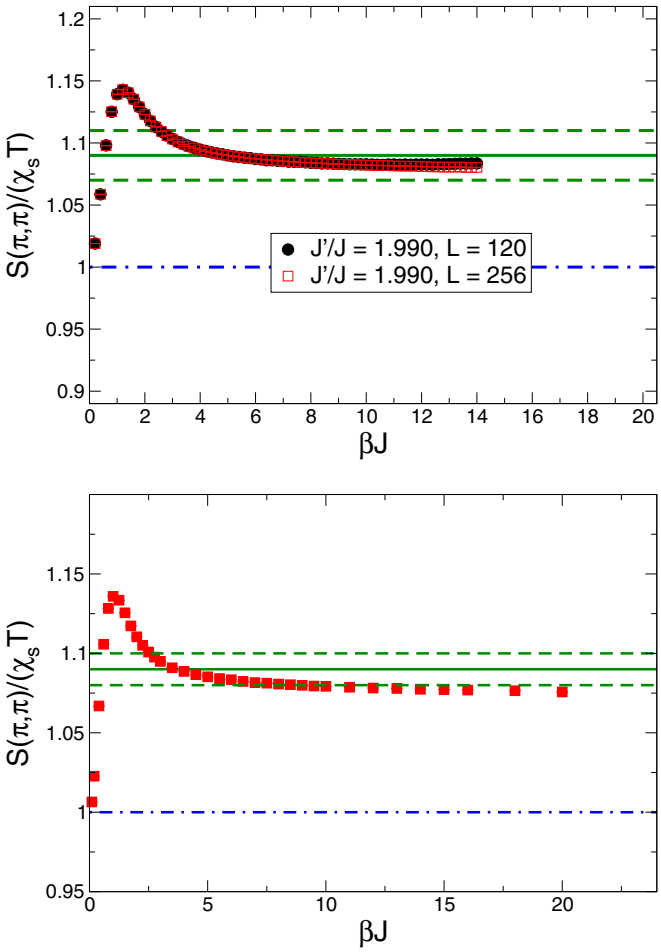

FIG. 13. $S(\pi,\pi)/(\chi_s T)$ as functions of β for the disordered model (top panel) and the clean dimerized system (bottom panel) investigated in this study. In both panels, data sets are determined at the corresponding critical points and the horizontal solid lines are the theoretical predictions 1.09. The data of $L = 120$ and 256 shown in the top panel indicate that most likely the outcomes associated with $L = 256$ are the bulk ones. Most of the results shown in the bottom panel are from the data of simulations with $L = 256$.

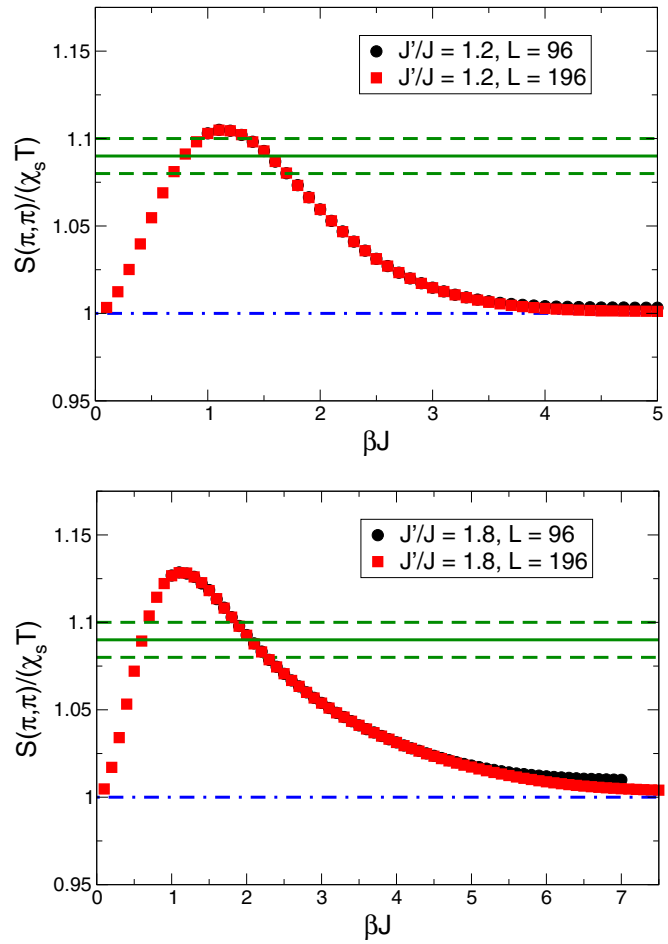

FIG. 14. $S(\pi,\pi)/(\chi_s T)$ as functions of β for the studied disordered model with $J'/J = 1.2$ (top panel) and $J'/J = 1.8$ (bottom panel). In both panels, the horizontal solid lines are the theoretical prediction 1.09. These results are calculated using 8000 (4000) MC sweeps for the thermalization (measurement).

understanding of its analytic expression. This is beyond the scope of our study presented here.

For the analysis done in the following (sub)sections, the assumption $z = 1$ will be employed.

C. Universal coefficient Ξ

Theoretically, a calculation with $z = 1$ for the $O(N)$ nonlinear sigma model using the large-N expansion predicts that up to the order of $1/N$, the quantity Ξ, which is defined as $S(\pi,\pi)/(\chi_s T)$, is a universal number given by 1.09 for $N = 3$ (which is the case here). The observables $S(\pi,\pi)/(\chi_s T)$ as functions of β for the considered models are shown in Fig. 13. In both panels of Fig. 13 the solid lines represent the theoretical value 1.09. In addition, an uncertainty of few percent (of 1.09, dashed lines) is included in both panels as well. The results shown in Fig. 13 imply that although non-negligible T dependence for $S(\pi,\pi)/(\chi_s T)$ does appear for these models, the Monte Carlo data agree very well with the associated theoretical predictions.

Most of the data shown in the bottom panel of Fig. 13, which are associated with the clean plaquette model, are determined from the results obtained on $L = 256$ lattices. For this model, we have performed simulations with $L = 256$ and 512 for the largest value of β considered ($\beta = 20$). The agreement between the results of $S(\pi,\pi)/(\chi_s T)$ obtained from these two calculations is remarkably good (the difference is only around one per mille). Therefore, the conclusion that our Monte Carlo data are consistent with the theoretical prediction is unquestionable.

Figure 13 also indicates that the data of $S(\pi,\pi)/(\chi_s T)$ of the considered two models approach 1.0 (dashed-dotted lines in both panels) at the regions of high temperature. This is consistent with the associated analytic calculations.

For the disordered model, in addition to the simulations performed close to the critical point, we have carried out calculations with $J'/J = 1.2$ and 1.8. The results of $S(\pi,\pi)/(\chi_s T)$ for $J'/J = 1.2$ and 1.8 are demonstrated in Fig. 14. As shown in the figure, no plateaus appear for these two newly obtained data sets of $S(\pi,\pi)/(\chi_s T)$. This implies

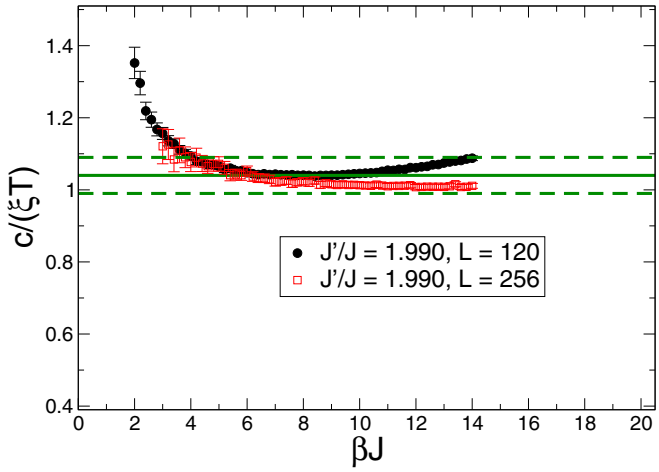

FIG. 15. $c/(T\xi)$ as functions of β for the disordered model investigated in this study. The data sets are determined at the corresponding critical point $(J'/J)_c = 1.990$ and the horizontal solid line is the theoretical prediction 1.04.

that the expected QCR behavior of this quantity does not show up when the calculations are conducted away from the associated QCP. This observed phenomenon is in agreement with the outcome determined in [19]. It is also interesting to find that at both the regions of high and low temperatures, the corresponding results of Ξ approach 1.0 (dashed-dotted lines in both panels of Fig. 14). This is again consistent with the expected theoretical prediction.

D. Universal coefficient X

The final universal coefficient studied here is associated with $c/(T\xi)$ and is predicted to be 1.04 in theory. For the investigated disordered system, the associated $L = 120$ and 256 data of $c/(T\xi)$ as functions of β are presented in Fig. 15. In the figure besides the data of $c/(T\xi)$, the related theoretical value and few percent error for it are also shown as the solid and dashed lines, respectively. Similar to the scenario found in our analysis of $S(\pi,\pi)/(\chi_s T)$, a noticeable dependence on T for the quantity $c/(\xi T)$ is observed. In addition, while the bulk results of the universal coefficient X are reached only for those with $\beta < 7.5$, it is likely that for $\beta \in [7.5, 9.0)$ the associated X are the bulk ones as well. Considering the fact that there is a broad range of β where the determined X are within the theoretical predicted value with a reasonable estimated error for it, the claim that our results shown in Fig. 15 are consistent with the outcomes conducted in Refs. [12,13,15] is unquestionable. While not shown here, a similar situation occurs when $c/(\xi T)$ of the clean dimerized plaquette model is considered. In particular, analogous finite-size and finite-temperature effects as those appearing in Fig. 15 are found.

IV. DISCUSSIONS AND CONCLUSIONS

Using the first-principles nonperturbative QMC simulations, we have investigated the exotic characteristics of QCR related to both a 2D quantum spin system with configurational disorder and a 2D clean dimerized spin-$\frac{1}{2}$ Heisenberg model. These unique properties of the considered models result from the interplay of the thermal and the quantum fluctuations. We first reconfirm that the dynamic exponent z for the disordered model studied here is 1. With this result, as well as the fact that $z = 1$ for the clean dimerized plaquette model, the three universal coefficients associated with QCR, namely, Ω, Ξ, and X are calculated. We find our Monte Carlo data of both the disordered and the clean systems are consistent with the analytic results based on the large-N calculations of the $O(N)$ nonlinear sigma model. It is interesting to notice that while quantum systems with certain kinds of quenched disorder, such as the configurational disorder employed in this study, violate the Harris criterion [22,30–33], 2D disordered spin-$\frac{1}{2}$ models with bond dilution fulfill this principle [25,34–37]. The results presented here seem to imply the scenario that disordered systems which violate the Harris criterion conform to the theoretical predictions of QCR. It will be compelling to investigate whether for models that satisfy the Harris criterion, the corresponding values of the three universal coefficients of QCR remain the same as the known ones in the literature.

While the numerical data obtained from the QMC simulations are in good agreement with the corresponding analytic predictions, non-negligible dependence on T is observed for these three universal coefficients. Furthermore, for both the considered models, the estimated values of Ω, which are related to $\chi_u c^2$, are different statistically from the analytic and numerical ones established in the literature (except those determined in Ref. [23]). The difference between the values of Ω estimated here [$\Omega = 0.306(10)$ or $\Omega = 0.32(1)$] and the theoretical result previously known ($\Omega \sim 0.27$) is more than 10 percent, which cannot be accounted for by the potential systematic uncertainties resulting from the calculations of c conducted in this study. Among the relevant studies associated with Ω, only the dedicated work of Ref. [23] agrees with ours. It is also interesting to notice that the Ω estimated in Ref. [23] is somewhat (slightly) larger than what has been calculated here. We attribute this to the fact that data with temperatures (lattice sizes) lower (larger) than ours were used in that work for the related analysis. Indeed, in our investigation with a fixed $z = 1$, the magnitude of Ω is increasing when more and more data of higher T are excluded in the fits. Aside from that, finite-temperature effect clearly shows up for $\chi_u c^2/T$, as can been seen in Figs. 8 and 11. Such an effect to some extent will influence the determination of Ω if the formula $\chi_u c^2 = \Omega T$ is used to extract the value of Ω.

It is intriguing that while the analytic outcome of Ω including both the leading and subleading contributions deviates significantly from its numerical estimations obtained in this study and in Ref. [23], the theoretical prediction of Ω by considering only the leading term is in better agreement with our results and that of Ref. [23]. In summary, the numerical evidence reached here for the described discrepancy is quite convincing. A detailed study of χ_u for the clean bilayer spin-$\frac{1}{2}$ model demonstrates such a deviation as well [23]. To shed light on this deviation, aside from conducting analytic studies associated with corrections not considered before, it will be desirable as well to simulate other disordered and clean dimerized models other than those investigated here.

ACKNOWLEDGMENTS

We thank A. W. Sandvik for bringing Ref. [23], in which a detailed investigation of Ω based on a clean bilayer spin model was conducted, to our attention. This study is partially supported by Ministry of Science and Technology of Taiwan.

[1] S. Chakravarty, B. I. Halperin, and D. R. Nelson, Phys. Rev. Lett. **60**, 1057 (1988).
[2] J. D. Reger and A. P. Young, Phys. Rev. B **37**, 5493 (1988).
[3] S. Chakravarty, B. I. Halperin, and D. R. Nelson, Phys. Rev. B **39**, 2344 (1989).
[4] J. Oitmaa, C. J. Hamer, and Zheng Weihong, Phys. Rev. B **50**, 3877 (1994).
[5] C. J. Hamer, Zheng Weihong, and J. Oitmaa, Phys. Rev. B **50**, 6877 (1994).
[6] U.-J. Wiese and H.-P. Ying, Z. Phys. B **93**, 147 (1994).
[7] A. W. Sandvik and D. J. Scalapino, Phys. Rev. B **51**, 9403 (1995).
[8] B. B. Beard and U.-J. Wiese, Phys. Rev. Lett. **77**, 5130 (1996).
[9] A. W. Sandvik, Phys. Rev. B **56**, 11678 (1997).
[10] F.-J. Jiang, F. Kampfer, M. Nyfeler, and U.-J. Wiese, Phys. Rev. B **78**, 214406 (2008).
[11] F.-J. Jiang and U.-J. Wiese, Phys. Rev. B **83**, 155120 (2011).
[12] A. V. Chubukov and S. Sachdev, Phys. Rev. Lett. **71**, 169 (1993).
[13] A. V. Chubukov and S. Sachdev, Phys. Rev. Lett. **71**, 2680 (1993).
[14] A. Sokol, R. L. Glenister, and R. R. P. Singh, Phys. Rev. Lett. **72**, 1549 (1994).
[15] A. V. Chubukov, S. Sachdev, and J. Ye, Phys. Rev. B **49**, 11919 (1994).
[16] A. W. Sandvik, A. V. Chubukov, and S. Sachdev, Phys. Rev. B **51**, 16483 (1995)
[17] M. Troyer, H. Kontani, and K. Ueda, Phys. Rev. Lett. **76**, 3822 (1996).
[18] M. Troyer, M. Imada, and K. Ueda, J. Phys. Soc. Jpn. **66**, 2957 (1997).
[19] J.-K. Kim and M. Troyer, Phys. Rev. Lett. **80**, 2705 (1998).
[20] Y. J. Kim, R. J. Birgeneau, M. A. Kastner, Y. S. Lee, Y. Endoh, G. Shirane, and K. Yamada, Phys. Rev. B **60**, 3294 (1999).
[21] Y. J. Kim and R. J. Birgeneau, Phys. Rev. B **62**, 6378 (2000).
[22] D.-X. Yao, J. Gustafsson, E. W. Carlson, and A. W. Sandvik, Phys. Rev. B **82**, 172409 (2010).
[23] A. Sen, H. Suwa, and A. W. Sandvik, Phys. Rev. B **92**, 195145 (2015).
[24] A. W. Sandvik, Phys. Rev. B **59**, R14157(R) (1999).
[25] A. W. Sandvik, Phys. Rev. B **66**, 024418 (2002).
[26] The quantity ρ_s (spin stiffness) is defined as $\rho_s = \frac{1}{2\beta}\sum_{i=1,2}\langle W_i^2\rangle$, where W_i is the winding number in the spatial i direction.
[27] S. Wenzel and W. Janke, Phys. Rev. B **79**, 014410 (2009).
[28] F.-J. Jiang, Phys. Rev. B **83**, 024419 (2011).
[29] The $\chi_u c^2/T$ data of the clean plaquette model determined at $(J'/J)_c$ are examined carefully and indeed those shown in this study are size convergent. It is anticipated that the results associated with $J'/J = 1.8228$ and 1.8232 should be size convergent as well.
[30] Nvsen Ma, Anders W. Sandvik, and Dao-Xin Yao, Phys. Rev. B **90**, 104425 (2014).
[31] A. B. Harris, J. Phys. C: Solid State Phys. **7**, 1671 (1974).
[32] J. T. Chayes, L. Chayes, D. S. Fisher, and T. Spencer, Phys. Rev. Lett. **57**, 2999 (1986).
[33] O. Motrunich, S. C. Mau, D. A. Huse, and D. S. Fisher, Phys. Rev. B **61**, 1160 (2000).
[34] O. P. Vajk and M. Greven, Phys. Rev. Lett. **89**, 177202 (2002).
[35] R. Sknepnek, T. Vojta, and M. Vojta, Phys. Rev. Lett. **93**, 097201 (2004).
[36] R. Yu, T. Roscilde, and S. Haas, Phys. Rev. Lett. **94**, 197204 (2005).
[37] A. W. Sandvik, Phys. Rev. Lett. **96**, 207201 (2006).